

Comparison of Wearable Methods for Estimating Cardiac Timings: A Comprehensive Multimodal Echocardiography Investigation

Parastoo Dehkordi ^{1,§}, Farzad Khosrow-Khavar ^{2,§}, Marco Di Rienzo ³, Omer T. Inan ⁴, Samuel E. Schmidt ⁵, Andrew P. Blaber ⁶, Kasper Sørensen ⁵, Johannes J. Struijk ⁵, Vahid Zakeri ², Prospero Lombardi ³, Md. Mobashir H. Shandhi ⁴, Mojtaba Borairi ⁷, John M. Zanetti and Kouhyar Tavakolian ^{6,8,*}

¹Electrical and Computer Engineering Department, University of British Columbia Vancouver, BC, Canada

²Heart Force Medical Inc., BC, Canada

³IRCCS Fondazione Don Carlo Gnocchi, Milan, Italy

⁴School of Electrical and Computer Engineering, Georgia Institute of Technology, Georgia, USA

⁵Department of Health Science and Technology, Aalborg University, Aalborg, Denmark

⁶Department of Biomedical Physiology and Kinesiology, Simon Fraser University, BC, Canada

⁷Fraser Health Authorities, Burnaby, BC, Canada

⁸Electrical Engineering Department, University of North Dakota, USA

[§]Parastoo Dehkordi and Farzad Khosrow-Khavar have contributed equally to this work

Correspondence*:

Kouhyar Tavakolian

kouhyar.tavakolian@enr.und.edu

2 ABSTRACT

3 Cardiac time intervals are important hemodynamic indices and provide information about left
4 ventricular performance. Phonocardiography (PCG), impedance cardiography (ICG), and recently,
5 seismocardiography (SCG) have been unobtrusive methods of choice for detection of cardiac
6 time intervals and have potentials to be integrated into wearable devices. The main purpose of
7 this study was to investigate the accuracy and precision of beat-to-beat extraction of cardiac
8 timings from the PCG, ICG and SCG recordings in comparison to multimodal echocardiography
9 (Doppler, TDI, and M-mode) as the gold clinical standard. Recordings were obtained from 86
10 healthy adults and in total 2120 cardiac cycles were analysed. For estimation of the pre-ejection
11 period (PEP), 43% of ICG annotations fell in the corresponding echocardiography ranges while

12 this was 86% for SCG. For estimation of the total systolic time (TST), these numbers were 43%,
13 80% and 90% for ICG, PCG, and SCG, respectively. In summary, SCG and PCG signals provided
14 an acceptable accuracy and precision in estimating cardiac timings, as compared to ICG.

15 **Keywords:** Cardiac time intervals, phonocardiography (PCG), impedance cardiography (ICG), seismocardiography (SCG), echocardi-
16 ography, pre-ejection period (PEP), left ventricular ejection time (LVET)

1 INTRODUCTION

17 Cardiac time intervals have clinical significance in mitral valve stenosis, coronary artery disease (? , ?),
18 arterial hypertension (?), atrial fibrillation, hypovolemia and fluid responsiveness (?), chronic myocardial
19 disease (?) and in the assessment of left ventricular performance (? , ?). These intervals present a temporal
20 description of the sequential phases of a cardiac cycle. Some of the important cardiac intervals include
21 pre-ejection period (PEP), defined as the time period between the onset of left ventricular depolarization
22 (the onset of QRS complex on electrocardiogram (ECG), and in particular the ECG Q wave when available)
23 and the opening of the aortic valve (?); left ventricular ejection time (LVET), defined as the interval between
24 aortic valve opening and closure events; total systolic time (TST), defined as the time between ECG Q and
25 the closure of the aortic valve; and electromechanical delay (EMD), defined as the time interval between
26 ECG Q and the closure of the mitral valve (? , ?). Estimation of cardiac intervals involves detecting the
27 timing of the opening and closure of the aortic and mitral valves.

28 In clinical settings, the opening and closure of the aortic and mitral valves are commonly measured
29 noninvasively using different ultrasound modalities such as M-mode, Doppler flow imaging, Tissue
30 Doppler Imaging (TDI) or speckle tracking strains. These methods are time-consuming and require a
31 trained sonographer to obtain accurate cardiac images. As such, there is a growing interest in the search
32 for alternative simpler techniques to measure cardiac intervals. Phonocardiography (PCG), impedance
33 cardiography (ICG) and seismocardiography (SCG) have been extensively used for this purpose (Figure ??).
34 The non-invasive nature of these technologies makes them well-suited for inclusion in wearable solutions
35 (? , ? , ? , ?). This paper provides a unique and comprehensive analysis of the accuracy of cardiac timings
36 estimated using PCG, ICG and SCG recordings, as compared to standard echocardiography methods.

37 1.1 Background

38 PCG is the measure of the heart sounds and is captured using a stethoscope and microphone. These
39 sounds are generated by valve closure as well as by blood flow turbulence during systole and diastole. In a
40 normal heart, two dominant sounds, S1 and S2, appear in rhythmical form (?). S1, the first heart sound,
41 occurs when the mitral valve closes (the start of systole). S2, the second heart sound, occurs at the end of
42 systole and is related to the closure of the aortic valve. By determining the beginning of S1 and S2 on the
43 PCG signals, and the onset of QRS wave on ECG, EMD and TST intervals can be estimated. Since PCG
44 signals do not contain information related to the opening of the aortic valve, PEP cannot be extracted from
45 the PCG recordings (see Figure ??).

46 ICG is a technology which measures the thoracic impedance. During each cardiac cycle, the change
47 in blood volume of the thoracic arterial system, results in a change in the electrical conductivity and the
48 impedance of the thorax. The impedance changes are primarily due to changes in the velocity and volume
49 of the blood in the aorta (? , ?). The fiducial points on the first derivative of an impedance waveform (B
50 and X), have been proposed to coincide with aortic valve opening and closure, respectively, making it
51 possible to measure LVET, which was subsequently used to estimate stroke volume and other hemodynamic

52 parameters (see Figure ??). In addition, there have been subsequent efforts to use ICG independently to
53 approximate PEP (?, ?).

54 SCG captures the chest acceleration induced by the motion of myocardium recorded using an accelero-
55 meter commonly mounted on the lower part of the sternum. In 1957, SCG was recorded under the name
56 of precordial ballistocardiogram (?) and was used in the early 1960s for monitoring heart rate variability
57 (?). Afterward, in the late 1980s, SCG was introduced as a technology for monitoring cardiac function
58 (?). In a study conducted by ?, the fiducial points of SCG, labeled as MC, AO, AC and MO were found
59 to correspond to mitral valve closure, aortic valve opening, aortic valve closure and mitral valve opening,
60 respectively, and validated against the echocardiography images (?). Recently, Sørensen et al. conducted a
61 study to define fiducial points in the SCG recordings obtained from forty-five healthy individuals (?). In
62 each subject the SCG waveforms were averaged and the points were then correlated with the cardiac events
63 identified in ultrasound images.

64 The main purpose of our study was to provide a comprehensive validation of the accuracy of cardiac inte-
65 rvals estimated using PCG, ICG and SCG, as compared to the measurements made using echocardiography.
66 An international team of researchers with expertise in non-invasive cardio-mechanical signals annotated
67 the fiducial points on PCG, ICG and SCG recordings and estimated the cardiac intervals with respect to
68 ECG Q. Later, we compared these estimates with the echocardiographic measures of the same cycles.

69 This study extended previous studies with the following aspects: 1) the simultaneous recording of PCG,
70 ICG and SCG which made it possible to compare the cardiac interval estimates from three different methods
71 ; 2) the recruitment of a larger number of participants (eighty-six individuals); 3) beat-to-beat annotation
72 of fiducial points without ensemble averaging over cardiac cycle. Averaging may remove the beat to beat
73 variations and could introduce errors due to changes in heart rate; as such, every individual cardiac cycle
74 was annotated separately leading to the analysis of more than two thousand separate cardiac cycles; 4) the
75 use of multimodal echocardiography, M-mode, Doppler and TDI; 5) suggesting a new method to measure
76 the heart valve opening and closure using electrocardiography. While echocardiography is commonly used
77 in clinical cardiology for annotating the timing of the cardiac valve opening and closure and measuring
78 cardiac intervals, it has its own imprecisions mostly induced by the intrinsic noise of the images and the
79 lack of agreement between the measurements of different sonographers. To address this issue we suggested
80 a new and different measurement protocol introducing valve opening and closing time ranges. Rather than
81 associating each valve movement with a single time instant, the timing of the valve opening or closure
82 event was associated with a time window ranging from the initiation to the completion of the event; and, 6)
83 The annotations for each different technology of ICG, PCG and SCG were performed by experts in each
84 field and not a single group.

2 MATERIALS AND METHODS

85 2.1 Participants

86 Eighty five healthy, male and female ($n = 51$) adults between 19-85 years of age (age: 27.8 ± 10.3 , BMI:
87 24.2 ± 5.00) were recruited for this study. Subjects with known history of cardiovascular, respiratory, or
88 major musculoskeletal injuries were excluded from recording. The participants were initially scanned with
89 echocardiography to detect any visible cardiac anomalies including valvular regurgitations and pre-existing
90 congenital heart disease.

91 This study was carried out in accordance with the recommendations of Simon Fraser University policies
92 and procedures involving human participants with written informed consent from all subjects. All subjects

93 gave written informed consent in accordance with the Declaration of Helsinki. The protocol was approved
94 by the Office of Research Ethics at Simon Fraser University, Vancouver, Canada.

95 **2.2 Data Acquisition**

96 Two pairs of ICG sensors were placed on the neck and on the mid-axillary line at the xiphoid process
97 level to measure the ICG signals (BoMed Inc., NCCOM3, USA). A low-noise 3-axial MEMS joint
98 accelerometer-gyroscope sensor (ASC GmbH, ASC IMU 7.002LN.0750, Germany) was used to record
99 SCG. The sensor was mounted on the sternum close to the xiphoid process and secured by double-sided
100 tape. The PCG signals were recorded using a digital stethoscope mounted on the middle of sternum
101 (Thinklabs digital stethoscope, CO, USA). Simultaneously, a reference two-lead ECG (iWorx Systems,
102 Inc., IX-BIO8-SA, NH, USA) was recorded. All recordings were conducted with iWorx data acquisition
103 system (iWorx Systems, Inc., IX-416, NH, USA), sampled at 1000 Hz with 16-bit resolution.

104 A Vivid q portable ultrasound machine (GE Medical Systems, New York, US) was used for recording
105 echocardiograms. To synchronize between the iWorx data acquisition system and echocardiography
106 machine, separate ECG signals were used as input to these machines and their electrodes were placed close
107 to each other on the shoulders to create more similarity in ECG morphologies.

108 All data recordings were performed at the Aerospace Physiology Lab at Simon Fraser University, Canada.

109 **2.3 Echocardiography Protocol**

110 Echocardiography is a standard modality extensively used in clinical settings for a variety of diagnostic
111 purposes. However, its accuracy in finding the exact instant of valve opening or closing, besides being
112 affected by noise and operator variability, as mentioned in the background section, it is also limited by the
113 resolution of the captured frame and its poor synchrony with the ECG (?). To overcome these imprecisions,
114 we proposed a new protocol for recording and labelling the echocardiogram images by performing a
115 multimodal echocardiographic procedure and considering time windows for the assessment of the valve
116 openings and closures. To avoid artifacts in the signals subjects underwent an echocardiographic scan in
117 the supine position. If necessary, participants were only slightly tilted to the left lateral position to improve
118 the quality of echocardiography.

119 **2.3.1 Multimodal Echocardiography**

120 **M-mode.** M-mode was used to demonstrate the excursion of the aortic valve cusps (Figure ??). To
121 improve the quality of images, special attention was taken to choose the angle through which the M-mode
122 cursor was placed on the valve at a specific plane of cut. The M-mode images were not sufficiently accurate
123 for measuring mitral valve opening and closure due to ambiguities produced by highly vibrating thin floppy
124 leaflets attached to chordal apparatus.

125 For M-mode, in many cases the ascending aorta showed a steep upward motion in systole and returned to
126 its original position in diastole taking the cusps out of the focused region. This made it impossible to detect
127 both the aortic valve opening and closure in the same cardiac cycle (second cycle in Figure ??). For these
128 cycles, only the aortic valve opening, or closure was labelled.

129 **Doppler Flow.** Doppler Flow was used to acquire spectral flow Doppler of blood across the aortic valve
130 in apical-5 or apical-3 chamber views, whichever was more parallel to the flow across the valve (Figure ??).
131 To optimize the spectral Doppler flow images for measuring the timing of aortic events, special attention
132 was given to collect the sample flow from the center of the flow jet through the central proximal region of
133 the ascending aorta. To avoid attenuation of the images by lung tissues in the supine position, for some
134 participants the Doppler flow images were acquired at the end of exhalation.

135 **TDI.** TDI was used to measure myocardium velocity during each cardiac cycle by placing the sample
136 volume in the ventricular myocardium immediately adjacent to the mitral annulus in apical four-chamber
137 view. This relatively new modality of the echocardiogram technique allowed the time intervals of the aortic
138 and mitral valves to be measured with increased consistency (Figure ??).

139 2.3.2 Valve Opening and Closure Ranges

140 Since the valve opening and closure occurs over a period from the initiation of the event until the
141 completion point, rather than reporting a single time, we reported a time range for each event. As such,
142 for the aortic valve, using the M-mode modality, the initial time of opening and the full opening of the
143 cusps were labelled as AVO_{min} and AVO_{max} , respectively (Figure ??). The same for aortic valve closure,
144 AVC_{min} was marked as the initiation of the closing aortic cusps and AVC_{max} was marked at the exact
145 instant after the complete closure of the cusps.

146 On the Doppler flow images, the AVO_{min} was labelled as the moment before the blood flow (no-flow-yet
147 point); the AVO_{max} was annotated as the moment when the blood flow was observed. AVC_{min} was marked
148 as the point before the blood flow stopped and AVC_{max} was marked at the point after that there was no
149 blood flowing (Figure ??).

150 On TDI images, the AVO_{min} was marked at the exact moment before the annulus descended toward the
151 apex and the AVO_{max} was labelled as the point when the annulus started descending toward the apex. At
152 the end of systole, the myocardium reaches negative velocity. As the open aortic valve suddenly closes,
153 there is a slight bounce, resulting in a shift from negative to positive velocity; AVC_{min} and AVC_{max} were
154 marked respectively as the exact moments before and after the bounce (Figure ??). As well, the exact
155 moment before the annulus ascended away from the apex (when the myocardium velocity shifted from
156 positive to negative) was labelled as MVO_{min} . The exact moment after the annulus had started ascending
157 away from the apex was labelled as MVO_{max} (Figure ??). MVC was always annotated as a single point
158 annotation, rather than a range like the other points (Figure ??).

159 2.4 Manual Annotations of ICG, SCG and PCG

160 Cardiac timings are traditionally defined relative to the onset of ECG QRS complex, which is considered
161 as the starting point of cardiac contraction. However, for some subjects the start of QRS (Q-wave) was not
162 easy to be detected. In these cases, we started with the neighboring R-wave and used the valley immediately
163 located before the Q-wave.

164 Estimation of cardiac intervals from the ICG signal required annotation of the characteristic points of B
165 and X, which are assumed to coincide with the opening and closing of the aortic valve. In this study, ICG
166 B was annotated as the local minimum on the notch to the left of point C (Figure ??) and the X point was
167 annotated as the time instant where the lowest ICG value occurred after point C (?). PEP_{icg} was measured
168 as the interval from ECG Q to ICG B and TST_{icg} was obtained as the interval from ECG Q to ICG X.
169 LVET was calculated as the timing interval between B and X points.

170 On PCG signals, the S1 and S2 sounds were annotated by the expert; EMD_{pcg} and TST_{pcg} were estimated
171 as the interval from the ECG Q to the beginning of S1 and S2, respectively. The onset of the S1 sound was
172 defined as the onset of the first peak after the ECG Q which had a height that exceeds the max amplitude of
173 the preceding diastolic period. The onset of the S2 sound was defined as the onset of the first sharp negative
174 wave in the S2 sound.

175 It was proposed that the SCG fiducial points of MC, MO, AC and AO would coincide with mitral
176 valve and aortic valve closing and opening, respectively. For the annotation of these points the traditional
177 nomenclature proposed by Crow et al was considered (?). On this basis, PEP_{scg} was obtained from ECG Q

178 to the SCG AO point and TST_{scg} was measured from ECG Q to the SCG AC point (Figure ??). EMD_{scg}
 179 and $Q-MO_{scg}$ were measured as the intervals from ECG Q to the SCG MC and MO points, respectively.
 180 $LVET_{scg}$ was measured as the time interval between SCG AO and SCG AC.

181 2.5 Statistical Analysis

182 Accuracy was assessed as the difference of the SCG, PCG and ICG measurements with respect to echocar-
 183 diography measurements. All the results were presented for every individual modality of echocardiography
 184 (M-mode, Doppler and TDI) and also for all cycles from all modalities together.

185 The percentage of cycles where the ICG, PCG, or SCG annotated fiducial points fell inside the,
 186 5-millisecond margins of, corresponding echocardiography ranges were reported. The choice of a
 187 5-millisecond margin was due to the time resolution limitations of the GE Vivid q system.

188 PEP estimation error (err_{pep}) were calculated using the following equation:

$$err_{pep} = 100 * \frac{abs(PEP_{ref} - PEP_{est})}{PEP_{ref}} \quad (1)$$

189 where PEP_{est} represents PEP_{icg} or PEP_{scg} and PEP_{ref} represents PEP_{mmode} , $PEP_{doppler}$ or PEP_{tdi} . PEP_{ref}
 190 was measured from ECG Q to the middle point of AVO_{min} to AVO_{max} . A similar formula to equation 1,
 191 was used to calculate the estimation error for ST, EMD and Q-MO.

192 The agreement between ICG, PCG and SCG estimated time intervals and the reference echocardiogram
 193 intervals, using the middle-point of the echocardiography range, were assessed using the multiple-
 194 observation Bland-Altman method (?). Bias, 95% limits of agreement (LOA) and two standard deviations
 195 (2SD) were reported to quantify the distributions of error.

196 In addition, the interclass correlation coefficient (ICC) was estimated as a reliability index. ICC reflects
 197 both the degree of correlation and the agreement between measurements. ICC was estimated as a ratio of
 198 reference variance over reference variance plus error variance. Based on the 95% confidence interval of the
 199 ICC estimate, values less than 0.5, between 0.5 and 0.75, between 0.75 and 0.9, and greater than 0.90 are
 200 indicative of poor, moderate, good, and excellent reliability, respectively (?).

201 Since the annotation of SCG, ICG and PCG fiducial points were manually performed by the different
 202 annotators, a separate independent annotator was trained to annotate all the same recordings of SCG,
 203 ICG and PCG. This was used to provide a quantification of annotator variability and evaluate the ease
 204 of annotation of fiducial points for every modality. ICC was estimated to show the agreement between
 205 annotators.

3 RESULTS

206 3.1 PEP measurements

207 M-mode was available for 85 participants, with a total of 504 measurements of AVO_{min} and AVO_{max} .
 208 Doppler flow was available for 59 participants giving a total of 292 cardiac cycles and TDI was available
 209 for 53 participants giving a total of 256 cardiac cycles. The average interval between AVO_{min} and AVO_{max}
 210 was estimated to be 19.3 ms, 16.4 ms and 14.7 ms for M-mode, Doppler and TDI, respectively.

211 The results for all PEP measurements are listed in Table ??. For 55% of cardiac cycles, ICG B points fell
 212 within M-mode AVO_{min} and AVO_{max} . Bias and 2SD between PEP_{icg} and PEP_{mmode} (the mid-point of
 213 echo range) were estimated as 11.7 ms and 29.24 ms, respectively. The average of error was estimated
 214 as 23.2% using Equation 1. For 83% of the cycles, the SCG AO fell within the M-mode AVO_{min} and

215 AVO_{max} range. The agreement between PEP_{scg} and PEP_{mmode} was assessed by the Bland-Altman method
216 with a bias of 2.1 ms and 2SD of 26.0 ms. The average of error was estimated as 12.5%.

217 The value of PEP_{echo} , PEP_{icg} and PEP_{scg} for all cycles were compared in Figure ???. For all echocardiography
218 measurements of AVO_{min} and AVO_{max} from M-mode, Doppler and TDI modalities, 47% of ICG
219 B and 86% of SCG AO occurred in their corresponding echocardiography ranges. The average percentage
220 error between PEP_{echo} and PEP_{icg} and PEP_{scg} were estimated at 25.5% and 12.8%, respectively. The
221 agreements between PEP_{echo} and PEP_{scg} and PEP_{icg} were assessed by the Bland-Altman plot (Figure ??).

222 3.2 TST measurements

223 The comparison between TST_{icg} , TST_{pcg} and TST_{scg} estimates and the corresponding measurements
224 from different echocardiography modalities are presented in Table ???. TST was the only timing parameter
225 that could be estimated by all three technologies (ICG, PCG and SCG). The values of TST_{echo} , TST_{icg} ,
226 TST_{scg} and TST_{pcg} for all cycles are depicted in Figure ???. For all cardiac cycles, 43%, 90% and 80% of
227 annotated corresponding aortic valve closure points on ICG, PCG and SCG signals fell within the AVC
228 echocardiography range, respectively. The value of 2SD between TST_{echo} and TST_{icg} , TST_{pcg} and TST_{scg}
229 were calculated as 55.8 ms, 21.8 ms and 16.3 ms, respectively. ICC between TST_{echo} and TST_{icg} , TST_{pcg}
230 and TST_{scg} were estimated as 0.61, 0.94 and 0.97, respectively.

231 3.3 EMD and Q-MO measures

232 TDI images were used for measuring the timing of mitral valve opening and closure. The average EMD,
233 was calculated over 211 cardiac cycles, was 31.5 ± 7 ms using TDI echocardiography, 36.8 ± 9.7 ms using
234 PCG, and 31.9 ± 9.8 ms using SCG. For 46% of all cycles, PSG S1 fell in the 5 ms vicinity of MVC_{tdi}
235 while this value was 45% for MC_{scg} . The average of error between EMD_{scg} and EMD_{pcg} with EMD_{tdi}
236 were 24.0% and 28.5%, respectively.

237 For 44% of all the measurements, MO_{scg} fell within the MVO_{min} and MVO_{max} interval. The agreement
238 between MO_{scg} and MVO_{tdi} was assessed by a Bland-Altman analysis with the bias of -19.00 ms and the
239 2SD of 27.6 ms (Table ??).

240 3.4 LVET Measurements

241 For LVET measurements, we only used the TDI method which could provide reliable simultaneous
242 measurement of aortic valve opening and closure for 237 cardiac cycles. The measurement of LVET was
243 also provided from ICG and SCG by finding the B to X interval for ICG and AO to AC interval for SCG.
244 2SD between $LVET_{tdi}$ and $LVET_{icg}$ and $LVET_{scg}$ were estimated at 52.8 ms and 28.1 ms, respectively.
245 The biases were around 4 ms for both SCG and ICG. The percentage errors were 5.7% and 3.2%, and ICC
246 was 0.60 and 0.81, for ICG and SCG, respectively.

247 3.5 Between Annotator Variability

248 To measure the reliability between annotators, an independent person was trained to annotate all fiducial
249 points of ICG, PCG and SCG recordings. This annotator was blind to the results of echocardiography and
250 other annotators. ICC was estimated to measure the agreement between annotators. For ICG PEP and TST,
251 the ICC values between annotators were 0.45 and 0.76, respectively. The PEP and TST obtained from SCG,
252 the ICC between two annotators were 0.78 and 0.93. For PCG TST, the ICC values was 0.93.

4 DISCUSSION

253 The primary focus of this study was to investigate and quantify the reliability of the available non-
254 invasive methodologies with the potential to be embedded in wearable devices (ICG, SCG and PCG),
255 for detecting the clinically relevant cardiac timings. The results of this study can be used for informing

256 future development of wearable devices for ubiquitous assessment of cardiac timing intervals. These results
 257 suggest that acoustic (PCG) and vibration (SCG) signals are more precise and accurate, compared to ICG,
 258 for such applications. The findings of this study can be summarized as follow:

- 259 1. The PEP derived from ICG significantly deviates from the echocardiography range (for more than 50%
 260 of cycles) while the same parameter extracted from SCG was in the echocardiogram range for 86% of
 261 cycles.
- 262 2. TST_{pcg} and TST_{scg} estimation error were less than TST_{icg} estimation error; however, even for
 263 estimating TST_{icg} , these errors were small (about 6%), which could be negligible in some applications.
- 264 3. LVET estimation error was negligible for both ICG and SCG recording. However, the distribution of
 265 error (2SD) was almost twice as high for ICG.
- 266 4. EMD estimated from PCG and SCG recording delivered a very high average error accounting to about
 267 a quarter of the value of the interval itself. This could be totally in the margin of error of the GE Vivid
 268 q echocardiography device, and probably most other clinically available devices, making it difficult to
 269 draw a significant conclusion on this timing.
- 270 5. The variability between annotators was most significant in annotating the fiducial points on the ICG
 271 recordings.

272 The annotations of ICG, PCG and SCG were undertaken by an international group of experts. These
 273 timings were compared with the same timings measured using three different echocardiography methods,
 274 currently used in the clinical practice (M-mode, Doppler and TDI). Rather than an absolute single assi-
 275 gnment for valve opening or closure, echocardiography time ranges were compared with. No ensemble
 276 averaging was used and individual annotation of more than 2120 cardiac cycles was undertaken. Ensemble
 277 averaging could smooth the outliers and possibly improve the results. However, in a real clinical setting
 278 where the measurements are only available for a few cycles, if not a single cycle, ensemble averaging is not
 279 possible. Moreover, the variation of heart rate could affect the performance of ensemble averaging.

280 **ICG:** In only 47% of cycles, ICG B occurred in the echocardiography AVO range and PEP_{icg} , on average,
 281 differed by about 25% from PEP_{echo} . Revisiting the initial claims for correspondence of the B point to
 282 aortic valve opening (?) takes us to two echocardiography papers from 1980s. The first paper (?) included
 283 only a single plot of M-mode and ICG together and did not have any quantitative comparison between the
 284 measurements. The second paper (?), only provided results for LVET and indicated that ICG estimates
 285 over-estimates the echo measurement.

286 Compared to PEP estimation, $LVET_{icg}$ and TST_{icg} both provided better estimates for LVET and TST
 287 with only 5.7% and 6% deviation from the echocardiography measurements. This lower deviation is
 288 to be expected. Since LVET is a much longer period than PEP, a small deviation from echo would not
 289 change the percentage error as much as it would for PEP. This adequate approximation of LVET was the
 290 reason it was used in the formula for estimation of stroke volume (?). However, this could have created
 291 a misunderstanding, from early on, that the start of the LVET is also an independent reliable timing,
 292 corresponding to PEP. Neither our current results nor any results from previous studies - of which we are
 293 aware - quantitatively prove this supposition. There is a recent effort reporting similar results, as in this
 294 paper, when it comes to ICG (?).

295 **PCG:** The TST interval was measured using PCG with a negligible average error of 2.1%. However, the
 296 EMD estimation error was 24%. There was also a bias of 4.3 ms between EMD_{pcg} and EMD_{tdi} , showing

297 that EMD_{pcg} has been overestimated by 5.1 ms on average. Considering the short duration of EMD this
298 contributed to a significant error in the estimation of mitral valve closure.

299 **SCG:** For 86% of the cycles, SCG AO took place in the echocardiography AVO range. For PEP_{scg}
300 estimation, the average error was about 12.8%. For ST_{scg} estimation error was 1.4% on average. The
301 annotated AC point on the SCG recordings provided very close estimates to the echocardiography AVC
302 measures. These results were in line with a recent study on the SCG signal (?). For EMD_{scg} the average
303 error was about 21.7%, almost the same as EMD_{pcg} .

304 The Q-MO had an average difference of 4.6% with echo Q-MO and on average occurred 19 ms behind
305 the echo measurement. This bias was expected and matched with the original research, conducted by ?,
306 which compared echocardiogram with SCG and reported the worst diastolic timing at MO.

307 **Different Echocardiography Methods:** From Tables ?? and ?? no significant difference between ICG,
308 SCG and PCG is observed when it comes to the modality of the echocardiography. The same relation holds
309 using either M-mode, Doppler or TDI.

310 **Between Annotator Variability:** The ICC was the highest for TST extraction using both PCG and SCG,
311 indicating the ease of training someone to annotate the point. The PEP extraction was challenging; this can
312 be seen in lower ICC values for both ICG and SCG. The EMD values had ICC of 0.78, which is a higher
313 value with respect to PEP.

314 The estimation of cardiac time intervals using PCG, SCG and ICG, investigated in this study, offers an
315 opportunity to assess cardiac contractility which, in addition to the analysis of the other features of these
316 signals, broadens the potential of SCG, PCG and ICG in the monitoring of cardiovascular performance.
317 As these technologies yield themselves to wearable applications, they could be used outside of the
318 hospital/clinical settings to detect the potential abnormalities and malfunctions of the cardiovascular system
319 such as heart failure (?), hypovolemia (?), and hypotension (?) or to validate cardiac resynchronization
320 therapy (?). Moreover, this technology can be used to monitor the improvement of cardiac performance in
321 healthy individuals as the result of the adoption of a healthier and more active lifestyle.

322 In this study, we strictly limited the subject population to healthy people and avoided any cardiac
323 abnormalities. Cardiomyopathies clearly affect the morphology of ICG, PCG and SCG signals. Thus, the
324 next step for this study would be to include subjects with various cardiovascular diseases to evaluate the
325 methods further and to develop robust methodologies for fiducial point detection in such populations. It
326 should also be noticed that in this study the signals were manually annotated. Automatic annotation of
327 ICG, PCG or SCG recordings has its own challenges addressed in several studies. It should also be noted
328 that in all the annotations the simultaneous ECG signal was considered as the reference of the annotations.

329 The GE Vivid q device used in this study is regularly used in clinical environments and hospitals. However,
330 there is an inherent dis-synchrony between recorded images and the ECG signal obtained in the most
331 ultrasound devices. Assuming a similar error for ICG, SCG and PCG we do not believe such errors could
332 change the relations of the obtained results with each other. However, a research grade ultrasound device
333 could reduce such errors in future studies.

334 This study was limited to analysis of the z-axis of the accelerometer signal in the dorsoventral direction.
335 The movement of the chest due to cardiac vibration is not limited to this direction; the manifests itself
336 in the other two axes and also in rotational movements which can be picked up by Gyroscopes (?).
337 These additional signals were also recorded and, in the near future, we will analyze them to investigate

338 the possibility of using all aspects of the vibrations to reduce the error between echocardiography and
339 mechanical vibration annotations.

CONFLICT OF INTEREST STATEMENT

340 Parastoo Dehkordi and Vahid Zakeri are employed by Heart Force Medical Inc., Vancouver, Canada.
341 Kouhyar Tavakolian is on the Board of Directors at Heart Force Medical, Inc. Vancouver, Canada. Farzad
342 Khosrow-khavar is the CTO of Heart Force Medical Inc., Vancouver, Canada. The authors declare that they
343 don't have any non-financial competing interest.

AUTHOR CONTRIBUTIONS

344 P.D. contributed to design the study, data acquisition and processed the obtained data, analyzed the results,
345 prepared the figures and revised the paper critically for content. F.K. contributed to the design of the study
346 and revised the paper critically for content. A.B. revised the paper critically for content and helped with
347 data acquisition. V.Z. assisted with SCG annotations, and critically revising the report's content. M.B. is
348 the certified sonographer who conducted echocardiography, annotated the echocardiogram. M.D.R., P.L.,
349 and P.D. annotated SCG cycles and read over and edited the manuscript. O.I. and M.S. annotated ICG
350 cycles and read over and edited the manuscript. S.S., J.J.S. and K.S. annotated PCG cycles, read the paper
351 and provided feedback. J.Z. contributed to the design of the study. He passed away on November 29th,
352 2017. K.T. initiated the study, contributed to the design of the study, data acquisition and processed the
353 obtained data, analysed the results and drafted the reviews.

ACKNOWLEDGMENTS

354 The authors would like to thank Adrien Leathley, Nima Yazdi and Teresa Zhao for their collaboration and
355 assistance with data acquisition, and Sean Ross for helping to revise this manuscript.

REFERENCES

- 356 Badano, L. P., Gaddi, O., Peraldo, C., Lupi, G., Sitges, M., Parthenakis, F., et al. (2007). Left ventricular
357 electromechanical delay in patients with heart failure and normal qrs duration and in patients with right
358 and left bundle branch block. *Europace* 9, 41–47
- 359 Baevskii, R. M., Egorov, A. D., and Kazarian, L. A. (1964). The Method of Seismocardiography.
360 *Kardiologiia* 18, 87–89
- 361 Berka, C., Levendowski, D. J., Cvetinovic, M. M., Petrovic, M. M., Davis, G., Lumicao, M. N., et al.
362 (2004). Real-time analysis of eeg indexes of alertness, cognition, and memory acquired with a wireless
363 eeg headset. *International Journal of Human-Computer Interaction* 17, 151–170
- 364 Bernstein, D. P. and Lemmens, H. (2005). Stroke volume equation for impedance cardiography. *Medical
365 and Biological Engineering and Computing* 43, 443–450
- 366 Bland, J. M. and Altman, D. (1986). Statistical methods for assessing agreement between two methods of
367 clinical measurement. *The lancet* 327, 307–310
- 368 Boudoulas, H. (1990). Systolic time intervals. *European Heart Journal* 11, 93–104. doi:10.1093/eurheartj/
369 11.suppl_1.93
- 370 Brubakk, O., Pedersen, T. R., and Overskeid, K. (1987). Noninvasive evaluation of the effect of timolol on
371 left ventricular performance after myocardial infarction and the consequence for prognosis. *Journal of
372 the American College of Cardiology* 9, 155–160
- 373 Burlingame, J., Ohana, P., Aaronoff, M., and Seto, T. (2013). Noninvasive cardiac monitoring in pregnancy:
374 impedance cardiography versus echocardiography. *Journal of Perinatology* 33, 675–680

- 375 Carvalho, P., Paiva, R., Couceiro, R., Henriques, J., Antunes, M., Quintal, I., et al. (2010). Comparison of
376 systolic time interval measurement modalities for portable devices. In *Engineering in Medicine and*
377 *Biology Society (EMBC), 2010 Annual International Conference of the IEEE (IEEE)*, 606–609
- 378 Carvalho, P., Paiva, R. P., Henriques, J., Antunes, M., Quintal, I., and Muehlsteff, J. (2011). Robust
379 characteristic points for icg-definition and comparative analysis. In *BIOSIGNALS*. 161–168
- 380 Chen, G., Imtiaz, S. A., Aguilar-Pelaez, E., and Rodriguez-Villegas, E. (2015). Algorithm for heart rate
381 extraction in a novel wearable acoustic sensor. *Healthcare technology letters* 2, 28–33
- 382 Crow, R. S., Hannan, P., Jacobs, D., Hedquist, L., and Salerno, D. M. (1994a). Relationship between
383 seismocardiogram and echocardiogram for events in the cardiac cycle. *American journal of noninvasive*
384 *cardiology* 8, 39–46
- 385 Crow, R. S., Hannan, P., Jacobs, D., Hedquist, L., and Salerno, D. M. (1994b). Relationship between
386 seismocardiogram and echocardiogram for events in the cardiac cycle. *American journal of noninvasive*
387 *cardiology* 8, 39–46
- 388 Di Rienzo, M., Vaini, E., Castiglioni, P., Lombardi, P., Meriggi, P., and Rizzo, F. (2014). A textile-based
389 wearable system for the prolonged assessment of cardiac mechanics in daily life. In *Engineering in*
390 *Medicine and Biology Society (EMBC), 2014 36th Annual International Conference of the IEEE (IEEE)*,
391 6896–6898
- 392 Di Rienzo, M., Vaini, E., Castiglioni, P., Merati, G., Meriggi, P., Parati, G., et al. (2013). Wearable
393 seismocardiography: Towards a beat-by-beat assessment of cardiac mechanics in ambulant subjects.
394 *Autonomic Neuroscience* 178, 50–59
- 395 Granados, J., Tavera, F., Velázquez, J., López, G., Hernández, R., and Morales, A. (2015). Acoustic
396 heart. interpretation of phonocardiograms by computer. In *Journal of Physics: Conference Series (IOP*
397 *Publishing)*, vol. 582, 012057
- 398 Henry, I., Bernstein, D., Banet, M., Mulligan, J., Moulton, S., Grudic, G., et al. (2011). Body-worn, non-
399 invasive sensor for monitoring stroke volume, cardiac output and cardiovascular reserve. In *Proceedings*
400 *of the 2nd Conference on Wireless Health (ACM)*, 26:1–26
- 401 Inan, O. T., Baran Pouyan, M., Javaid, A. Q., Dowling, S., Etemadi, M., Dorier, A., et al. (2018). Novel
402 wearable seismocardiography and machine learning algorithms can assess clinical status of heart failure
403 patients. *Circulation: Heart Failure* 11, e004313
- 404 Koo, T. K. and Li, M. Y. (2016). A guideline of selecting and reporting intraclass correlation coefficients
405 for reliability research. *Journal of chiropractic medicine* 15, 155–163
- 406 Marcus, F. I., Sorrell, V., Zanetti, J., Bosnos, M., Baweja, G., Perlick, D., et al. (2007). Accelerometer-
407 derived time intervals during various pacing modes in patients with biventricular pacemakers:
408 Comparison with normals. *Pacing and Clinical Electrophysiology* 30, 1476–1481
- 409 Mounsey, P. (1957). Praecordial ballistocardiography. *British heart journal* 19, 259–271
- 410 Noda, K., Endo, H., Kadosaka, T., Nakata, T., Watanabe, T., Terui, Y., et al. (2017). Comparison of
411 the measured pre-ejection periods and left ventricular ejection times between echocardiography and
412 impedance cardiography for optimizing cardiac resynchronization therapy. *Journal of arrhythmia* 33,
413 130–133
- 414 Que, C.-L., Kolmaga, C., Durand, L.-G., Kelly, S. M., and Macklem, P. T. (2002). Phonspirometry
415 for noninvasive measurement of ventilation: methodology and preliminary results. *Journal of applied*
416 *physiology* 93, 1515–1526
- 417 Reant, P., Dijos, M., Donal, E., Mignot, A., Ritter, P., Bordachar, P., et al. (2010). Systolic time intervals as
418 simple echocardiographic parameters of left ventricular systolic performance: correlation with ejection
419 fraction and longitudinal two-dimensional strain. *European Journal of Echocardiography* 11, 834–844

- 420 Ruiz, J. C. M., Rempfler, M., Seoane, F., and Lindecrantz, K. (2013). Textrode-enabled transthoracic ele-
 421 ctrical bioimpedance measurements-towards wearable applications of impedance cardiography. *Journal*
 422 *of Electrical Bioimpedance* 4, 45–50
- 423 Salerno, D. M. (1990). Seismocardiography: A new technique for recording cardiac vibrations. concept,
 424 method, and initial observations. *Journal of cardiovascular technology* 9, 111–118
- 425 Salerno, D. M. and Zanetti, J. (1991). Seismocardiography for monitoring changes in left ventricular
 426 function during ischemia. *Chest* 100, 991–993
- 427 Sherwood, A., Allen, M. T., Fahrenberg, J., Kelsey, R. M., Lovallo, W. R., and Van Doornen, L. J. (1990).
 428 Methodological guidelines for impedance cardiography. *Psychophysiology* 27, 1–23
- 429 Sørensen, K., Schmidt, S. E., Jensen, A. S., Sjøgaard, P., and Struijk, J. J. (2018). Definition of fiducial
 430 points in the normal seismocardiogram. *Scientific reports* 8, 15455
- 431 Stern, H., Wolf, G., and Belz, G. (1985). Comparative measurements of left ventricular ejection time by
 432 mechano-, echo-and electrical impedance cardiography. *Arzneimittel-Forschung* 35, 1582–1586
- 433 Tadi, M. J., Lehtonen, E., Saraste, A., Tuominen, J., Koskinen, J., Teräs, M., et al. (2017). Gyrocardiogra-
 434 phy: A new non-invasive monitoring method for the assessment of cardiac mechanics and the estimation
 435 of hemodynamic variables. *Scientific reports* 7, 6823
- 436 Tavakolian, K., Dumont, G. A., Houlton, G., and Blaber, A. P. (2014). Precordial vibrations provide
 437 noninvasive detection of early-stage hemorrhage. *Shock* 41, 91–96
- 438 Umar, F. and Leyva, F. (2012). Is the pre-ejection period key to predicting the response to cardiac
 439 resynchronization therapy? *Circulation Journal* 76, 590–590

FIGURE CAPTIONS

Table 1. Estimated cardiac timings compared to reference measured using the different modalities of echocardiography. The last column shows the percentage of estimated cardiac timings dropping in the 5-ms margins of corresponding echocardiography range.

Cardiac timing	Echocardiogram modality	2SD (ms)	Bias (ms)	ICC	Error%	(%) in Range
PEP _{scg}	M-mode	26.0	2.1	0.74	12.5 ± 12.0	83
	Doppler	21.5	0.5	0.83	10.9 ± 14.8	90
	TDI	23.2	3.7	0.82	13.1 ± 18.1	86
	All	24.7	2.5	0.59	12.8 ± 16.5	86
PEP _{icg}	M-mode	29.2	11.7	0.34	23.2 ± 17.4	55
	Doppler	28.7	12.5	0.46	22.9 ± 20.8	54
	TDI	31.9	15.7	0.60	29.0 ± 22.8	37
	All	30.1	13.5	0.35	25.5 ± 20.6	47
TST _{scg}	M-mode	13.6	-0.2	0.97	1.4 ± 1.1	92
	Doppler	14.8	7.6	0.91	2.4 ± 1.6	83
	TDI	15.7	-0.5	0.96	1.6 ± 1.3	92
	All	16.2	2.0	0.97	1.4 ± 3.2	90
TST _{icg}	M-mode	56.0	15.4	0.84	5.2 ± 6.3	52
	Doppler	66.0	25.6	0.65	8.0 ± 7.6	30
	TDI	51.6	13.5	0.83	4.9 ± 6.1	40
	All	55.8	17.8	0.61	6.0 ± 7.0	43
TST _{pcg}	M-mode	21.5	-3.4	0.93	2.0 ± 1.9	80
	Doppler	18.0	5.1	0.86	2.3 ± 1.6	82
	TDI	19.6	-3.3	0.95	2.1 ± 1.8	78
	All	21.8	-0.8	0.94	2.1 ± 1.8	80

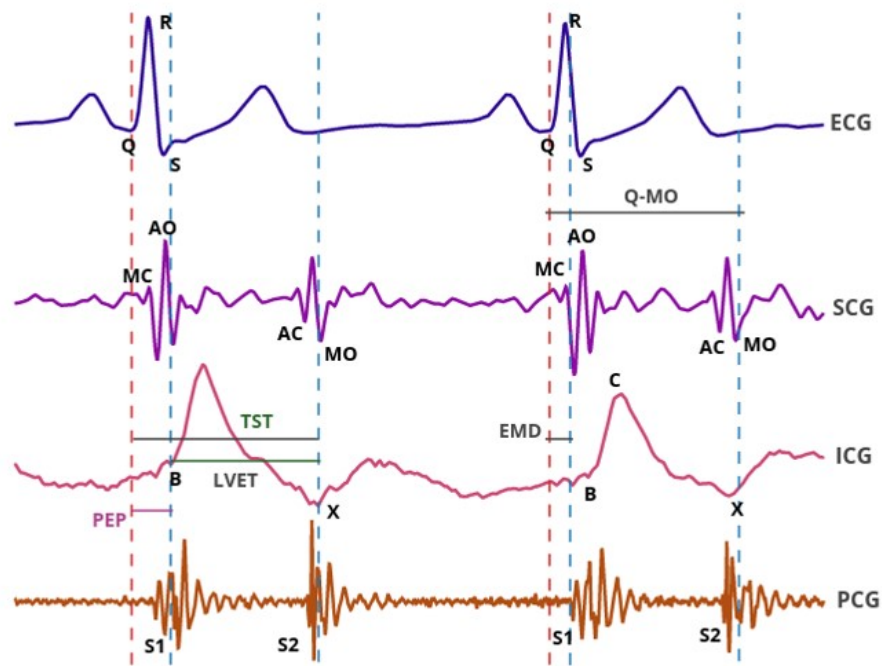


Figure 1. Simultaneous sample recordings of ECG, SCG, ICG, and PCG signals captured from a forty-year-old male participant in the supine position. The SCG MC and SCG MO points correspond to mitral valve closure and opening; the SCG AC and SCG AO points corresponded to the aortic valve closure and opening. ICG B point corresponded to aortic valve opening and ICG X point to aortic valve closure. EMD, PEP, TST and LVET systolic time intervals are also illustrated. S1 and S2 waves on PCG corresponded to mitral and aortic valve closure, respectively.

Table 2. The comparison of estimated EMD_{pcg} and EMD_{scg} compared to reference EMD_{echo} estimated using the TDI echocardiography and comparison of the SCG Q-MO intervals to the same intervals estimated from TDI images.

	2SD (ms)	Bias (ms)	In ranges (%)	Percentage Errors	ICC
EMD_{pcg}	18.0	4.3	46%	28.5 ± 29.9	0.59
EMD_{scg}	14.19	0.07	45%	24.0 ± 20.2	0.45
$Q-MO_{scg}$	27.62	-19.00	44%	4.6 ± 2.7	0.68

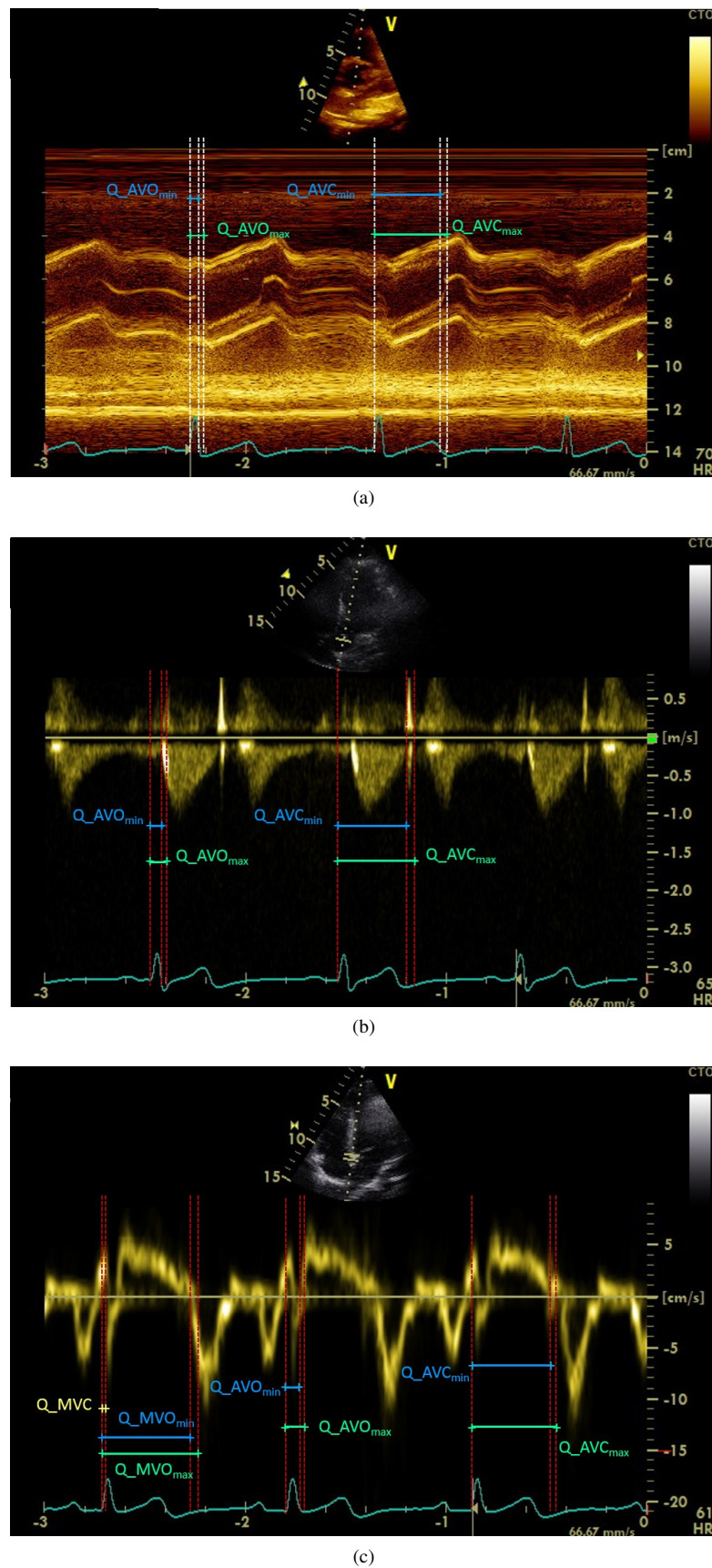


Figure 2. Echocardiogram images captured using (a) M-mode, (b) Doppler flow and (c) TDI modalities. AVO and AVC stand for aortic valve opening and closure. MVO and MVC stand for mitral valve opening and closure. Max and min subscripts represent the start and the end of the echocardiographic intervals.

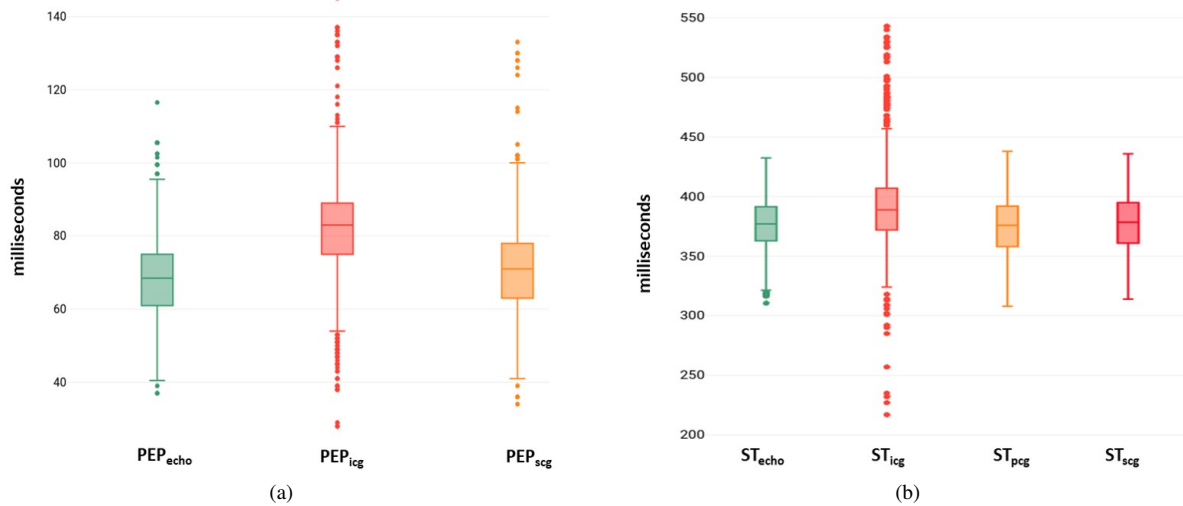


Figure 3. The boxplot shows the values of (a) PEP estimated from ICG and SCG and (a) TST estimated from ICG, PCG and SCG compared to the measurements from echocardiography. Lower quartile, median, and upper quartile values were displayed as bottom, middle, and top horizontal line of the boxes. Whiskers were used to represent the most extreme values within 1.5 times the interquartile range from the quartile. Outliers (data with values beyond the ends of the whiskers) were displayed as dots.

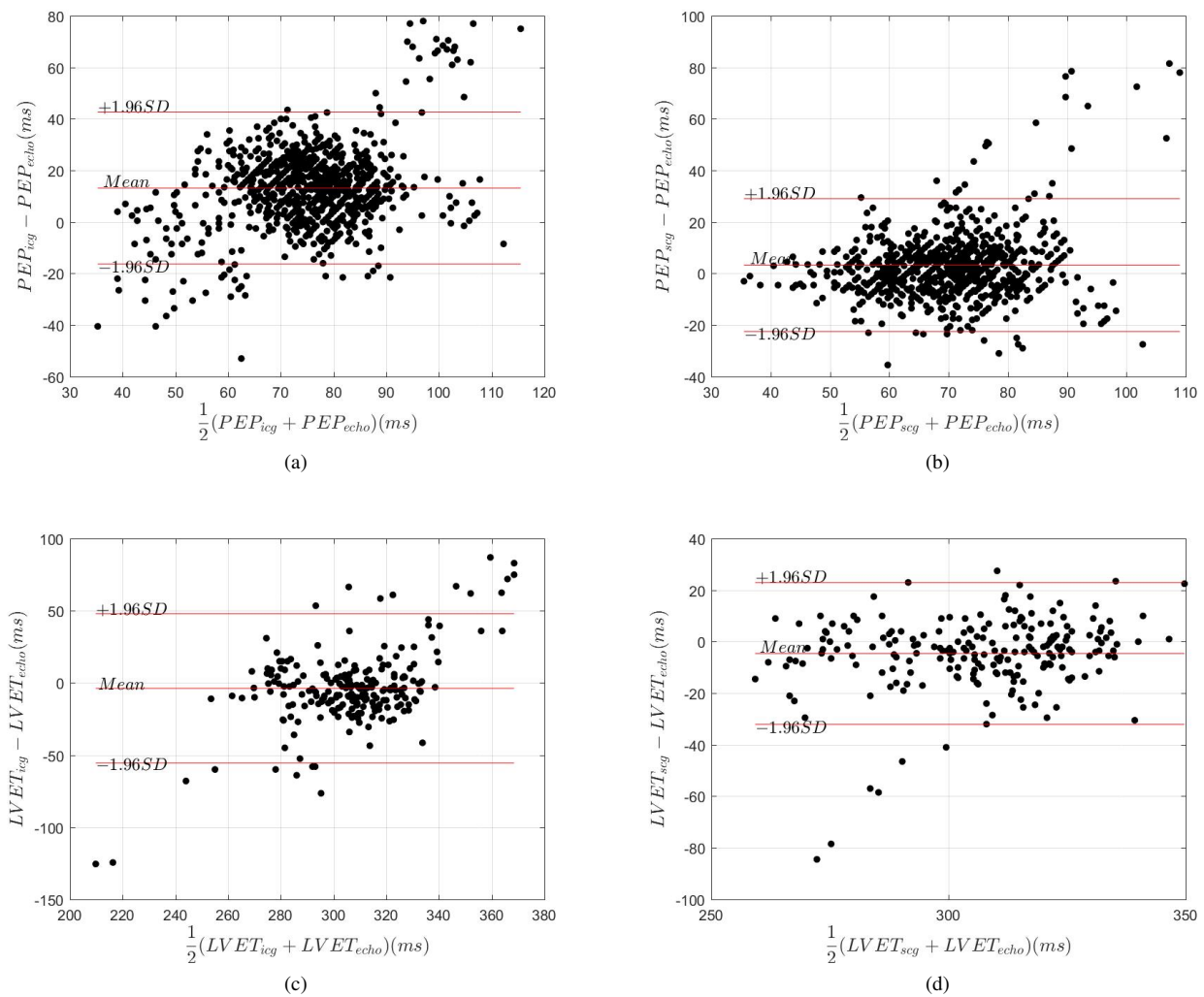


Figure 4. Bland and Altman plots for assessing the agreement between PEP_{echo} and (a) PEP_{icg} , (b) PEP_{scg} , and $LVET_{echo}$ and (c) $LVET_{icg}$, (d) $LVET_{scg}$.